Tellus (1978), *30*, 458–467

Boundary layer dynamics of a decaying vortex core

By WILLIAM H. RAYMOND and GANDIKOTA V. RAO, *Dept. of Earth and Atmospheric Sciences, Saint Louis University, P.O. Box 8099-Laclede Station, Saint Louis, Missouri 63156, U.S.A.*

(Manuscript received July 20, 1977; in final form February 8, 1978)

ABSTRACT

The rapid transient motions within a decaying axi-symmetric vortex boundary layer are analyzed for various "local" Rossby and Reynolds numbers. Both laminar (no-slip) and turbulent (slip) boundary conditions are considered for flows over rotating and stationary surfaces. Similarity transformations are performed by expanding the velocity components in powers of a ratio of dimensionless radius to time. The zeroth-order system described by two nonlinear second-order ordinary differential equations is solved by Newton's iterative method. Comparisons are made with Hatton (1975) for the special case of laminar flow over a stationary surface. For the first order system, asymptotic solutions representing the flow far above the lower surface are obtained.

For laminar flow our results indicate that the vertical velocity is either only downward, both upward and downward thus indicating the possibility of a stagnation point in the latter case or only upward motion depending on the value of the Rossby (Reynolds) number. Turbulent conditions are shown to produce only negative (downward) vertical velocities. The presence of an axial stagnation point and the value of the Reynolds number for which the axial motion (laminar, zeroth order) becomes completely downward corresponds with the findings of Hatton (1975). The addition of mass as simulated by blowing is shown to effectively delay the decay process.

1. Introduction

Studies of the boundary layers of concentrated atmospheric vortices: tornadoes, dust devils, etc., although simulated by many laboratory and theoretical investigations (for a review see Davies-Jones and Kessler, 1974), have faced numerous difficulties. These difficulties are primarily due to the fact that the tangential velocity profile in the free air changes radically with the radial distance, the governing partial differential equations are nonlinear, and the lower boundary conditions are hard to satisfy. Some of these vortices decay fast. The boundary layer dynamics within the inner portion of such rapidly decaying vortices is of interest in this study. Problems peculiar to the solution of decaying vortices include a knowledge of the initial velocity profiles and the relationship between the tangential velocity component and the radial pressure gradient and the nature of their time dependence. The decay of a vortex is characterized by the core expanding outward and the radial inflow becoming weakened. The outward expansion itself appears to be more a result of the internal flow dynamics than of diffusion.

The idealized inner core of such axisymmetric vortices is shown in Fig. 1 and is confined to a small radius r. The vertical axis is along z. The boundary layer is formed by the interaction of the vortex with the planar lower boundary and its vertical extent depends on Ω_s, the angular velocity of the lower surface. Along the z-axis the motion can be upward in the low levels and downward in the upper levels. The simultaneous existence of positive and negative vertical velocities results in stagnation at a point along the axis. This region is called the stagnation point region (Bellamy-Knights, 1974; Hatton, 1975). The viscous core region overlies the boundary layer. The decaying viscous core was studied earlier by Oseen (1911), Rott (1958, 1959) and Bellamy-Knights (1970, 1971). This core region is surrounded by potential flow which serves as an upper bound for the boundary layer flow at very large radii (Bellamy-Knights, 1974).

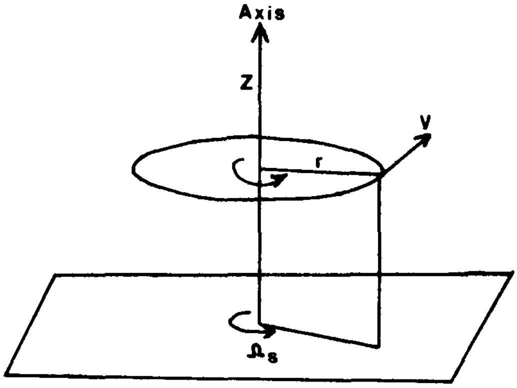

Fig. 1. The boundary layer of a vortex inner core of radius r. Ω_s is the angular velocity of the lower contact surface of the vortex. The vortex axis is along z and its tangential velocity is v.

Recent studies by Hatton (1975) of the boundary layer of a decaying vortex inner core showed that for laminar flow and solid rotation the axial motion can be up or down depending upon the value of a parameter proportional to the external angular velocity. Besides, an axial stagnation point was found provided there was radial inflow. The theoretical results were justified by appealing to the observational and laboratory findings (e.g., Rossman, 1960; Hoecker, 1960; Ward, 1972; Jischke and Parang, 1974; and see also Hsu and Fattahi, 1976).

In the following the governing Navier–Stokes equations, continuity and the two momentum equations, are written in dimensionless form and the flow variables are expressed in terms of a power series in r/t, an approach analogous to that suggested by Eliassen (1971). Here r and t are the dimensionless radial and time coordinates. A sufficient condition (not necessary) guaranteeing the validity of this approach is that the ratio r/t is smaller than 1. This places a major restriction on the region of the vortex investigated and the progression of time since the decay process began. This restriction will be clarified later.

The non-dimensionalization process introduces either the "local" Rossby number R_o or the Reynolds number R_e depending on whether we examine flow over a rotating or rigid surface, respectively. These numbers are defined as

$$R_e = V\delta\nu^{-1}, \tag{1a}$$

and

$$R_o = V\delta^{-1}\Omega_s^{-1} \tag{1b}$$

where V is the idealized tangential velocity observed at the top of the boundary layer, δ represents a characteristic depth, ν is the kinematic viscosity, and Ω_s is the angular velocity of the rotating solid lower boundary.

In this study the boundary layer dynamics are examined over a wide range of R_o or R_e numbers. Both laminar (no-slip) and turbulent (slip) boundary conditions are considered. For the case of laminar flow the first term approximation predicts an upward vertical motion and an axial stagnation point for a certain range of R_o (R_e). The same approximation for turbulent flow indicates the vertical flow to be downward. However, in both cases it was found that the fluid flow in the boundary layer and in the viscous vortex core far above the boundary are dependent upon the Rossby (Reynolds) number. The nature of these latter motions is predicted from the asymptotic solutions of the similarity equations. These asymptotes indicate that cyclostrophic balance (centrifugal force balancing the horizontal pressure gradient) is quickly attained for Rossby (Reynolds) numbers increasingly larger than one. Suitable similarity transformations are now presented.

2. The mathematical development

Consider an axisymmetric vortex of homogeneous and incompressible fluid with a fixed kinematic viscosity ν. Let this vortex be in contact with a plane boundary perpendicular to the axis of symmetry. Following a procedure similar to that used by Eliassen (1971) we express dimensional variables, denoted by a bar, in terms of V, Ω_s and δ and introduce the dimensionless variables r, z, t, m, u, w and the transformations:

$$\bar{t} = \Omega_s^{-1} t \quad \text{or} \quad \bar{t} = \delta^2 t \nu^{-1} \tag{2a}$$

depending on whether the flow is over a rotating or fixed lower surface, respectively and

$$\bar{r} = \delta r, \quad \bar{z} = \delta z, \quad \bar{m} = Vm\delta^{-1}, \quad \bar{u} = Vu, \bar{w} = Vw \tag{2b}$$

Here z denotes the vertical coordinate, r the radial distance from the vortex axis (a quantity that can greatly exceed one) and t the time while $m(r,z,t)$, $u(r,z,t)$ and $w(r,z,t)$ represent the angular, radial and vertical velocity components respectively. In addition, δ on a rotating surface is given by

$$\delta = \nu^{1/2}\Omega_s^{-1/2}$$

In terms of the dimensionless variables the governing Navier–Stokes equations representing flow over a rotating surface (for flow over a stationary surface replace R_o with R_e) are

$$\frac{\partial}{\partial r}(ru) + r\frac{\partial w}{\partial z} = 0 \tag{3a}$$

$$\frac{\partial mr^2}{\partial t} + R_o u\frac{\partial mr^2}{\partial r} + R_o w\frac{\partial mr^2}{\partial z} = \frac{\partial^2 mr^2}{\partial z^2} + \frac{r\,\partial^2 mr}{\partial r^2} + \frac{r\,\partial m}{\partial r} \tag{3b}$$

$$\frac{\partial u}{\partial t} + R_o u\frac{\partial u}{\partial r} + R_o w\frac{\partial u}{\partial z} + R_o(\Omega^2 - m^2)r = \frac{\partial^2 u}{\partial z^2} + \frac{\partial^2 u}{\partial r^2} + \frac{\partial}{\partial r}\left(\frac{u}{r}\right) \tag{3c}$$

for all r, z and $t > 0$. The first is the continuity equation which in combination with the two horizontal momentum eqs. (3b and 3c) determines the vertical velocity in the similarity solution. Hence the vertical momentum equation is not written separately. The nondimensional radial pressure gradient is expressed as $-\Omega^2 r$ in the last equation. As pointed out by Greenspan (1968) and Barrett (1975) the importance of the nonlinear terms is determined by the R_o or R_e numbers. In the early stages of decay these numbers are fairly large. Alternately, one may define $\tilde{u} = uR_o$, $\tilde{m} = mR_o$, $\tilde{w} = wR_o$ and $\tilde{\Omega} = \Omega R_o$ and rewrite eqs. (3a, b, c). For example the term $R_o(\Omega^2 - m^2)r$ becomes $(\tilde{\Omega}^2 - \tilde{m}^2)r$, and the equations do not show the explicit dependence on R_o. But the dependence remains implied through the parameter $\tilde{\Omega}$, used in describing the radial pressure gradient term.

The lower boundary conditions at $z = 0$ will depend upon whether the flow is laminar or turbulent. With the lower surface in solid rotation ($\tilde{m} = \Omega_s$) the laminar case requires that

$$m = R_o^{-1}, \quad u = W = 0 \tag{4}$$

at $z = 0$ for all $t > 0$. For the stationary case no-slip boundary conditions require that m is also zero. For the turbulent case the boundary conditions (Taylor, 1916), in dimensionless notation, are:

(on a rotating surface)

$$\frac{\partial m}{\partial z} = CR_o(m - R_o^{-1})[(m - R_o^{-1})^2 r^2 + u^2]^{1/2}$$

$$\frac{\partial u}{\partial z} = CR_o u[(m - R_o^{-1})^2 r^2 + u^2]^{1/2} \tag{5a}$$

(over a stationary surface)

$$\frac{\partial m}{\partial z} = CR_e m[m^2 r^2 + u^2]^{1/2}$$

$$\frac{\partial u}{\partial z} = CR_e u[m^2 r^2 + u^2]^{1/2} \tag{5b}$$

and $w = 0$. Here C is the dimensionless drag coefficient.

The exact expressions for the upper boundary conditions are to be determined from asymptotic solutions which are derived from, and are compatible with, the similarity equations. These asymptotic solutions are similar to the boundary conditions employed by Hatton (1975), see Section 5 and Appendix A for a detailed comparison. The flow overlying the boundary layer must approach cyclostrophic balance for high Rossby or Reynolds numbers. This condition may be expressed as $m(r, z \to \infty, t) \to \Omega(r, t)$ for large R_o or R_e. If the study of a decay of a vortex is contemplated when the initial state is represented by the steady-state the above condition is also a desirable initial condition at the beginning of the decay process. For Rossby (Reynolds) numbers of order one, transient terms in the equations assume importance so that deviation from the cyclostrophic balance exists. The following expressions are utilized after replacing z by $\eta(=z/2t^{1/2})$.

$$m(r,\eta,t) = t^{-1}[m_0(\eta) + rt^{-1}m_1(\eta) + \cdots]$$
$$u(r,\eta,t) = 2^{1/2}rt^{-1}[u_0(\eta) + rt^{-1}u_1(\eta) + \cdots]$$
$$w(r,\eta,t) = 2(2/t)^{1/2}[W_0(\eta) + rt^{-1}w_1(\eta) + \cdots]$$
$$\Omega(r,t) = t^{-1}[\Omega_0 + rt^{-1}\Omega_1 + \cdots] \tag{6}$$

A series of equations in various powers of r/t can be obtained by inserting (6) in eqs. (3). This procedure facilitates obtaining mathematical solutions relatively easily but their physical interpretation is somewhat complicated. Some of these equations along with the appropriate boundary conditions are now discussed.

3. The laminar boundary layer

3.1. *The equations—the zero-order system*

Substituting the above expressions into eqs. (3a, b, c) and collecting terms of the lowest power of r/t gives the zero-order system:

$$\begin{aligned} &2u_0 + w_0' = 0, \\ &-4u_0 - 2\eta u_0' \\ &\quad + 2(2)^{1/2}R_o(2u_0^2 + 2w_0u_0' + \Omega_0^2 - m_0^2) = u_0'' \\ &-4m_0 - 2\eta m_0' \\ &\quad + 4(2)^{1/2}R_o(2u_0m_0 + w_0m_0') = m_0'' \end{aligned} \tag{7}$$

The prime denotes differentiation with respect to η.

3.2. *The upper boundary conditions*

Upper boundary conditions are determined by assuming that m_0 and u_0 asymptotically approach constant respective values for η sufficiently large, i.e., z large or t very small. The asymptotes, as determined from the equations, are

$$m_0 = (\Omega_0^2 - \tfrac{1}{4}R_o^2)^{1/2} \quad \text{and} \quad u_0 = [2(2)^{1/2}R_o]^{-1} \tag{8}$$

We assume that in the limiting process (R_o or R_e large) $\bar{v}$ approaches V. This is equivalent to, via (2) and (6), requiring that m_0 approach Ω_0 the cyclostrophic condition for the zero-order system. In terms of the original variables the above expressions reduce to upper boundary conditions similar to those used by Hatton (1975). A comparison between Hatton's development of the decay problem and ours is given in Appendix A.

3.3. *The lower boundary conditions*

In the case of laminar flow the coupled ordinary differential eqs. (7) are complemented by lower boundary conditions derived from (4). The zero-order conditions are:
(on a rotating surface)

$$m_0 = R_o^{-1}, \quad u_0 = w_0 = 0 \quad \text{at} \quad \eta = 0$$

(on a stationary surface)

$$m_0 = u_0 = w_0 = 0 \quad \text{at} \quad \eta = 0.$$

4. Turbulent flow

The zero-order boundary conditions obtained from (5a, and b) for the turbulent flow are:

$$m_0' = 0, \quad u_0' = 0 \quad \text{and} \quad w_0 = 0 \quad \text{when} \quad \eta = 0 \tag{9}$$

The nonlinear system (7–9) has the following solution, which may or may not be unique:

$$m_0 = (\Omega_0^2 - \tfrac{1}{4}R_o^2)^{1/2}, \quad u_o = (22^{1/2}R_0)^{-1}$$

and

$$w_0 = -\eta/2^{1/2}R_o$$

These expressions are valid provided m_0 is well behaved, i.e.,

$$\Omega_0^2 - \frac{1}{4R_o^2} \geqslant 0$$

Note that a degenerate case occurs when $R_o = \frac{1}{2}\Omega_0$, i.e., $m_0 = 0$ but u_0 and $w_0 \neq 0$. The general solution represents a vortex in solid rotation with outward radial and downward vertical motions. The total contribution made by these terms to the boundary layer and viscous vortex depends upon the parameters Ω_0 and R_o. It should be noted that the horizontal velocity components near the top of the boundary layer for turbulent flow (zero-order solutions) are identical with the asymptotic zero-order solutions obtained under laminar conditions.

5. Flow near the top of the boundary layer

The asymptotic solutions of the first-order system will be determined for large η. Such solutions will be particularly interesting since they relate to non-solid rotation in the viscous vortex core. Their overall contribution is nevertheless small provided $rt^{-1}\,\Omega_1 \ll \Omega_0$. For large R_o, the restriction on rt^{-1} (given Ω_0, Ω_1, etc) is established by the expression

$$v = rt^{-1}\left(\Omega_0 + \frac{r}{t}\Omega_1 + \cdots\right) = 1$$

because we require that in the limiting process $\bar{v}$ approaches V.

5.1. *The first-order system*

Proceeding to the first-order system, obtained by substituting the series (6) into the eqs. (3a, b, c) and collecting terms in the next lowest powers of r/t, we obtain

$$\begin{aligned} &3u_1 + w_1' = 0 \\ &-8u_1 - 2\eta u_1' + 4(2)^{1/2} R_o(3u_0 u_1 \\ &\quad + w_0 u_1' + w_1 u_0' + \Omega_0 \Omega_1 - m_0 m_1) = u_1'' \\ &-8m_1 - 2\eta m_1' + 4(2)^{1/2} R_o(3u_0 m_1 \\ &\quad + w_0 m_1' + w_1 m_0' + 2u_1 m_0) = m_1'' \end{aligned} \tag{10}$$

There is no contribution made by the radial diffusion terms [i.e., radial terms on the right-hand side of eqs. (3b,c)] in the above system since they yield expressions of a different magnitude with respect to r/t.

5.2. *The asymptotic solutions*

Assuming that m_1 and u_1 approach constants provided η is sufficiently large, we can compute the asymptotes. They are

$$m_1 = \frac{\Omega_0 \Omega_1}{m_0 k} \tag{11}$$

and

$$u_1 = \frac{\Omega_0 \Omega_1}{4(2)^{1/2} R_o m_0^2 k}$$

where

$$k = 1 + \frac{1}{16 R_0^2 m_0^2}$$

For R_o large

$$k \approx 1$$

$$m_1 \approx \Omega_1$$

and

$$u_1 \approx 0.$$

5.3. *Zero- and first-order solutions combined*

Utilizing (11,8,6), we find that at the top of the boundary layer the motion is described by

$$v = \frac{r}{t}\left[m_0 + \frac{r}{t}\frac{\Omega_0\Omega_1}{m_0 k} + \cdots\right]$$

$$u = \frac{r}{t}\left[\frac{1}{2R_o} + \frac{r}{t}\frac{\Omega_0\Omega_1}{4R_o m_0^2 k} + \cdots\right] \tag{12}$$

and within this region the vertical velocity behaves as

$$w = -\frac{z}{t}\left[\frac{1}{R_o} + \frac{r}{t}\frac{3\Omega_0\Omega_1}{4R_o m_0^2 k} + \cdots\right]$$

Of course the actual or observed vertical velocity at the top of the boundary layer must also include the accumulated effect from the boundary layer. If the above expressions are related back to dimensional variables then we have (for flow over a rotating surface)

$$\bar{v} = R_o \frac{\bar{r}}{\bar{t}}\left[m_0 + \frac{R_o \bar{r}}{V\bar{t}}\frac{\Omega_0\Omega_1}{m_0 k} + \cdots\right]$$

$$\bar{u} = \frac{\bar{r}}{2\bar{t}}\left[1 + \frac{R_o \bar{r}}{V\bar{t}}\frac{\Omega_0\Omega_1}{2m_0^2 k} + \cdots\right]$$

$$\bar{w} = -\frac{\bar{z}}{\bar{t}}\left[1 + \frac{R_o \bar{r}}{V\bar{t}}\frac{3\Omega_0\Omega_1}{4m_0^2 k} + \cdots\right] \tag{13}$$

where m_0 is defined in (8). However, there is a restriction on the ratio $\bar{r}/\bar{t}$. It must satisfy

$$\frac{\bar{r}}{\bar{t}} = \frac{Vr}{R_o t}, \quad \text{or} \quad \frac{\bar{r}}{\bar{t}} = \frac{Vr}{R_e t}$$

depending on which lower boundary conditions are used. The restriction on r/t (Section 5) guarantees that $\bar{v}$ approaches V for R_o (R_e) increasingly large. Similar expressions also describe $\bar{z}/\bar{t}$. Clearly the magnitude of the ratio of V over R_o or V over R_e is established (initially) once Ω_s, δ, and ν are assigned values. Note the identities

$$V/R_o = (\nu\Omega_s)^{1/2} \quad \text{and} \quad V/R_e = \nu/\delta.$$

We can now compare eq. (13), the solutions at the top of the boundary layer, with the corresponding flow variables used by Hatton (1975): They are

$$\bar{V} = K_c \bar{r}/4\nu\bar{t}, \quad \bar{u} = \bar{r}/2\bar{t} \tag{14}$$

and

$$w = -\bar{z}/\bar{t}$$

where $2\pi K_c$ denotes the circulation. No restrictions were placed on $\bar{r}/\bar{t}$ or $\bar{z}/\bar{t}$. Other comparisons are given in Appendix A.

6. A numerical method

An effective numerical method for solving the boundary value problem described by eq. (7) and the boundary conditions enumerated in Section 3 in Newton's method (Keller, 1968). This iterative technique permits an efficient application of the Gaussian elimination procedure. All solutions for the finite difference equivalent of (7) are obtained using a constant step size of $\Delta\eta = 0.01$. Other details of the computations included the fact that w_0 was recalculated during each iteration using a Gaussian integration procedure. The convergence criteria required that the new calculations of u_0 and m_0 change by less than 10^{-4}. There was no difficulty in obtaining convergence for all cases tested. The initial guess first used was the steady-state solution due to Boedewadt (1940). The value chosen for Ω_0 was one. Interpolation for other values of Ω_0 is easily accomplished by using the relationships described in Section 2, i.e., for a specified $\tilde{\Omega}(\tilde{\Omega} = R_o\Omega)$, various combinations of R_o and Ω are possible.

The upper boundary conditions are reformulated using an approach suggested by Froese (1962). That is, the boundary conditions are replaced by the expressions

$$u_0^{N+1} = c_i u_0^N \quad \text{and} \quad m_0^{N+1} = c_2 m_o^N$$

implying that between discrete points η_N and η_{N+1} the values of u_0 and m_0 change by fixed amounts, c_1, and c_2, respectively. The values of c_1 and c_2 can be obtained from the asymptotic solutions. We choose $c_1 = c_2 = 1$ since it is known that for sufficiently large values of η, the independent variable, both m_0 and u_0 approach a constant.

7. Discussion of laminar results

Figs. 2, 3 and 4 respectively show the numerical solutions for the dimensionless vertical, radial and angular velocity fields (zero-order) for selected Rossby numbers $R_o = 1.6$, 5.0 and 500. The variation of vertical velocity as a function of R_o is apparent in Fig. 2. For example, the direction of the axial flow is entirely upward for large R_o's, like 500, and completely downward when R_o is less than or equal to 1.6. For a limited range of R_o; e.g., $1.6 < R_o < 10$ an axial stagnation point is observed.

Because the variation of R_o influences the solution greatly, we conjecture that no similarity solution of an unsteady vortex for a constant R_o is valid over a broad time period. Even though the

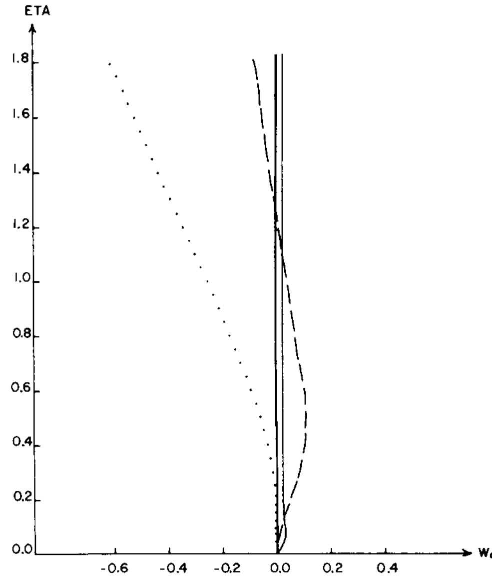

Fig. 2. Nondimensional measure of the zero order vertical component w_0. The solid, dashed and dotted lines represent the measures of w_0 for $R_o = 500$, 5 and 1.6 respectively.

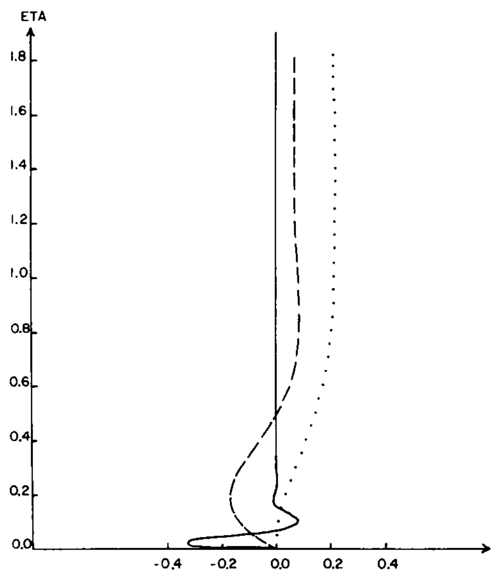

Fig. 3. Same as Fig. 2 except the radial component (u_0) is shown.

entire decay of the vortex core cannot be simulated using a single R_o, several distinct R_o's corresponding to discrete time periods may be employed. Hence η may be thought of as a vertical coordinate

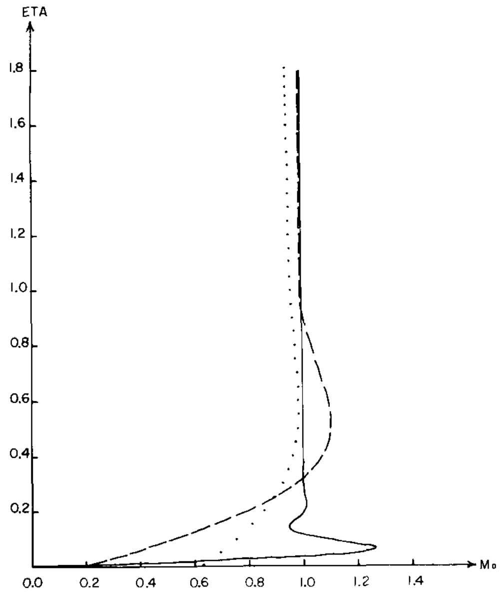

Fig. 4. Same as Fig. 2 except the angular velocity (m_0) is shown.

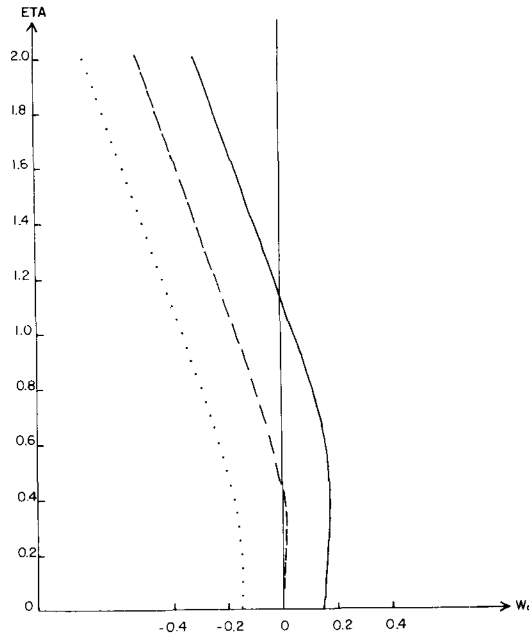

Fig. 5. Nondimensional vertical components, w_0's, illustrating the influence of blowing or suction for $R_0 = 2.0$. The solid, dashed and dotted lines represent w_0's respectively for blowing ($h_0 = 0.15$), neutral ($h_0 = 0$) and suction ($h_0 = -0.15$).

since we limit the range or value of t (remembering the restriction on r/t in Section 5). Alternately, z can be held fixed, and variations in η can be interpreted to have been caused by the changes in time. Thus, as Hatton (1975) has indicated, the precise significance of η and how the choices of z, t and r/t should be related to the physical situation is somewhat unclear. A greater observational knowledge of the meterological vortex should pave the way for an exact choice.

The depth of the boundary layer, the region below that η (interpreting η as a vertical coordinate) where u_0 and m_0, respectively, reach their asymptotic values given by eq. (8), can be easily identified in Figs. 3 and 4. Clearly the boundary layer is depressed when $R_o = 500$. At this Rossby number a large inflow region exists just above the lower boundary but the dimensionless radial velocity component very quickly approaches 0.707×10^{-3}, the asymptotic value for η larger than 0.2. When R_0 is decreased sufficiently ($R_0 < 1.6$) the entire boundary layer is composed of an outward directed radial velocity. From a kinematic point of view such an outflow contributes to the rapid deterioration in the final or decaying stage of a vortex.

In Fig. 4 we see that the angular velocities' deviation from the cyclostrophic condition that $m_0 = \Omega_0$ with $\Omega_0 = 1$ at the top of the boundary layer, is small even for $R_0 = 1.6$. Significant overshooting of the angular velocity occurs for large Rossby numbers, when the solutions contain oscillations resembling the steady-state profiles which were first given by Boedewadt (1940).

Fig. 5 illustrates how the vertical velocity is affected when the lower boundary condition $w_0 = 0$ is replaced with $w_0 = h_0$. Physically this is equivalent to replacing the solid rotating lower surface with a perforated boundary through which mass is added by blowing ($h_0 > 0$) or mass is removed by suction ($h_0 < 0$). The effect of blowing is to increase the depth of the axial upflow and effectively delay the decay process by intensifying the radial inflow. Just the opposite effect is observed for suction.

Numerical solutions for flow over a stationary surface, a more geophysically realistic problem, are given in Figs. 6, 7 and 8 for Reynolds numbers $R_e = 0.755$, 3.0, and 200. The dimensionless vertical velocity shown in Fig. 6 is characterized by flow which ranges from totally upward ($R_e = 200$) to flow entirely downward for $R_e \leqslant 0.755$. A stag-

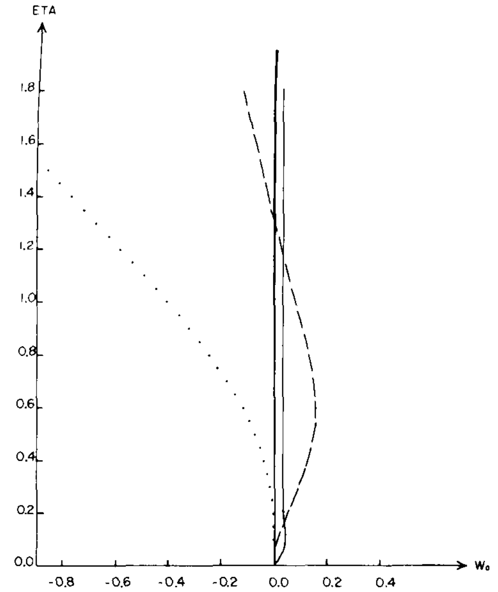

Fig. 6. Same as Fig. 2 except R_o is replaced by the nearly corresponding values of R_e.

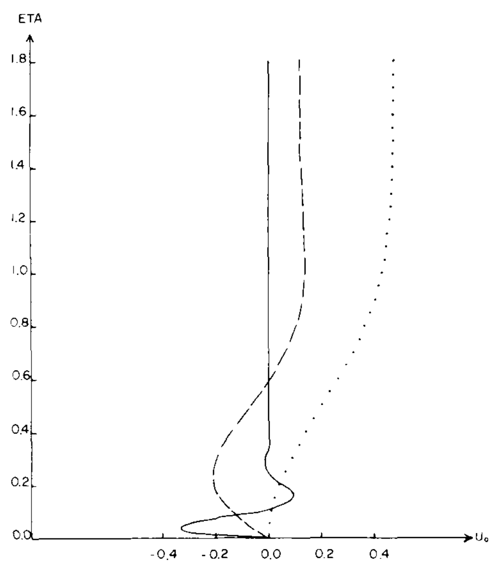

Fig. 7. Same as Fig. 3 except for the corresponding values of R_e.

nation point exists near the top of the boundary layer when $R_e = 3.0$.

Figs. 7 and 8 show the dimensionless radial and angular velocities, respectively. These exhibit behavior very similar to those displayed in Figs. 3 and 4: the major differences are the occurrence of radial inflow for $R_e > 0.755$ and the departure from the cyclostrophic balance ($m_0 = 1$) at the smaller Reynolds number.

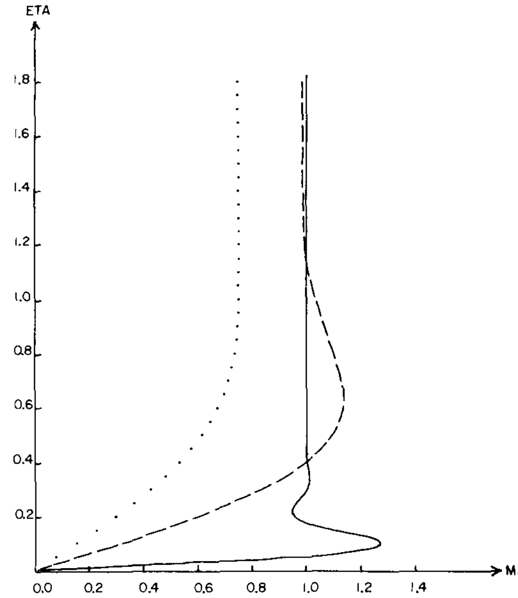

Fig. 8. Same as Fig. 4 except for the corresponding values of R_e.

8. Conclusions

Our findings show that a stagnation point, as described by Hatton (1975), does occur, during the decay process, within the boundary layer of a vortex core having laminar flow, but only for a limited range of R_0, or R_e's. On the other hand, according to the analytical discussion in Section 4, turbulent conditions produce only negative vertical velocities. Ward (1972) postulated that the enlargement observed on a dissipating tornadic funnel represents the transition zone between turbulent flow with negative vertical velocity and the laminar flow, nearest the surface, with its positive vertical motion. Our study gives credence to Ward's speculation on the differences in the direction of the vertical velocity between laminar and turbulent flows. These findings, however, are valid for a relatively short time period typical of the transient decay stage of a vortex.

We have also implied that the outward radial expansion of a vortex or vortex boundary layer during its final stage, once established, is due to the internal dynamics much more than purely diffusionary processes. However, our findings show that this tendency can be slowed or reversed by adding mass as modeled, or simulated, by blowing in this study.

In the final conclusion, we note that the velocity profiles are highly dependent upon the value of R_o (R_e). This is equivalent, in our study, to acknowledging the fact that initial conditions are very important when analyzing non-steady vortices.

9. Appendix A

9.1. *A comparison of the similarity transformations used in this study and those due to Hatton (1975)*

The first term in our series can be compared with the similarity transformations used by Hatton (1975). Using (1a), (2) and (6) we obtain the following expressions (first term only) for the dimensional velocity components (for flow over a fixed surface)

$$\bar{v} = R_e \frac{\bar{r}}{\bar{t}} m_0(\eta)$$

$$\bar{u} = 2^{1/2} R_e \frac{\bar{r}}{\bar{t}} u_0(\eta)$$

and

$$\bar{w} = 2(2)^{1/2} R_e \left(\frac{r}{\bar{t}}\right)^{1/2} w_0(\eta)$$

Hatton used the following similarity transformations: (we have changed his notation slightly for comparison purposes)

$$\bar{v} = \frac{\Omega_H \bar{r}}{4\bar{t}} G(\eta)$$

$$\bar{u} = \frac{\bar{r}}{2\bar{t}} F(\eta)$$

and

$$\bar{w} = -2\left(\frac{r}{\bar{t}}\right)^{1/2} H(\eta), \quad \left(\frac{dH}{d\eta} = F\right), \tag{A2}$$

where $\eta = z/2t^{1/2}$ or in terms of dimensional variables $\eta = \bar{z}/2\,(r\bar{t})^{1/2}$.

This suggests the following relationships:

$$F = 2(2)^{1/2} R_e u_0 \tag{A4}$$

$$G = 4R_e m_0/\Omega_H \tag{A4}$$

$$H = -(2)^{1/2} R_e w_0 \tag{A5}$$

To obtain the equations used by Hatton it is only necessary to redefine Ω_0^2 by

$$\Omega_0^2 \equiv \frac{\Omega_H^2}{16R_e^2} + \frac{1}{4R_e^2} \tag{A6}$$

a condition that also follows naturally from (A4) using the asymptotic values of G and m_0, i.e., $G = 1$ and $m_0 = \Omega_0^2 - \frac{1}{4}R_e^2)^{1/2}$. These equations may be obtained from (7) using (A3–6), they are:

$$F'' + 2\eta F' + 4F - 2F^2 + 4HF' + \frac{\Omega_H^2}{2}(G^2 - 1) = 2$$

$$G'' + 2\eta G' + 4G + 4HG' - 4FG = 0 \tag{A7}$$

and

$$H' - F = 0.$$

The critical value of Ω_H^2, where the vertical velocity is entirely downward, was found by Hatton to be $\Omega_H^2 = 4.952$. From (A6) we find that

$$R_e^2 = (\Omega_H^2 + 4)/16, \quad \text{if} \quad \Omega_0 = 1$$

and, for $\Omega_H^2 = 4.952$, we obtain the value of $R_e = 0.748$, a quantity reasonably close to our value of $R_e = 0.755$. The slight difference of 0.007 is probably due to the type of numerical method and to the step size used.

REFERENCES

Barrett, K. E. 1975. Numerical study of the flow between rotating coaxial discs. *Z. angew. Math. Phys.* **26**, 807–817.

Bellamy-Knights, P. G. 1970. An unsteady two-cell vortex solution of the Navier–Stokes equations. *J. F. M. 41*, 673–687.

Bellamy-Knights, P. G. 1971. Unsteady multicellular viscous vortices. *J. F. M. 50*, 1–16.

Bellamy-Knights, P. G. 1974. An axisymmetric boundary layer solution for an unsteady vortex above a plane. *Tellus 3*, 318–324.

Boedewadt, von U. T. 1940. Die Drehströmung über festem Grunde. *Z. angew Math. Mech. 20*, 241–253.

Davies-Jones, R. P. and Kessler, E. 1974. Tornadoes. *Weather and Climate Modification*, (edited by W. N. Hess). Wiley (See Chap. 16).

Eliassen, A. 1971. On the Ekman layer in a circular vortex. *J. Met. Soc. Japan 49*, 209–214.

Froese, C. 1962. On solving $y'' = fy - g$ with a boundary condition at infinity. *Math. Comp. 16*, 492–494.

Greenspan, H. P. 1968. *The Theory of Rotating Fluids*. Cambridge at the University Press.

Hatton, L. 1975. Stagnation point flow in a vortex core. *Tellus 27*, 269–279.

Hoecker, W. H. 1960. Wind speed and airflow patterns in the Dallas tornado of 2nd April 1957. *M. W. R. 88*, 167.

Hsu, C. T. and Fattahi, B. 1976. Mechanism of tornado funnel formation. *Physics of Fluids 19*, 1853–1857.

Jischke, M. C. and Parang, M. 1974. Properties of simulated tornado like vortices. *J. Atmos. Sci. 31*, 506–512.

Keller, H. B. 1968. *Numerical Methods for Two Point Boundary Value Problems*. Blaisdell Publishing Co.

Oseen, C. W. 1911. *Ark. f. Math., Astron. och Fys. 7*.

Rossman, F. O. 1960. On the physics of tornadoes. In: *Cumulus Dynamics*, Pergamon Press, Oxford.

Rott, N. 1958. On the viscous core of a line vortex. *Z. angew Math. Phys. 9b*, 543–553.

Rott, N. 1959. On the viscous core of a line vortex, II. *Z. angew. Math. Phys. 10*, 73–81.

Taylor, G. I. 1916. Skin friction of the wind on the earth's surface. *Proc. Roy. Soc. A*, *XCII*, 196.

Ward, N. B. 1972. The exploration of certain features of tornado dynamics using a laboratory model. *J. Atmos. Sci. 29*, 1194–1204.

ДИНАМИКА ПОГРАНИЧНОГО СЛОЯ В ЯДРЕ ЗАТУХАЮЩЕГО ВИХРЯ

Для различных значений "локальных" чисел Россби и Рейнольдса анализируются быстрые переходные процессы внутри пограничного слоя затухающего осесимметричного вихря. Для потоков над вращающимися и стационарными поверхностями рассматриваются как ламинарные (без проскальзывания), так и турбулентные (с проскальзыванием) граничные условия. Разложением компонент скорости по степеням отношения безразмерных радиуса и времени выполнены преобразования подобия. Система нулевого порядкаа, описываемая двумя обыкновенными нелинейными дифференциальными уравнениями второго порядка, решается итерационным методом Ньютона. Для специального случая ламинарного потока над стационарной поверхностью проведено сопоставление с результатами Хэттона (1975). Для системы первого порядка получены асимптотические решения, описывающие течение вдали над нижней поверхностью.

Для ламинарных течений наши результаты показывают, что вертикальные скорости направлены только вниз, или вверх и вниз, что в последнем случае указывает на возможность появления точки застоя, а также только вверх— в зависимости от числа Россби (Рейнольдса). Турбулентные условия ведут только к отрицательным вертикальным скоростям (направленным вниз). Наличие точки застоя на оси и величина числа Рейнольдса, для которого аксиальное движение (ламинарное и нулевого порядка) становится направленным только вниз, сответствуют результатам Хэттона (1975). Показано, что введение массы, моделируемое вдуванием, эффективно задерживает процесс затухания виря.